This microfiche was produced according to ANSI/AIIM Standards and meets the quality specifications contained therein. A poor blowback image is the result of the characteristics of the original document.

NASA-CR-200046

BUBBLE MASS CENTER AND FLUID FEEDBACK FORCE FLUCTUATIONS ACTIVATED BY CONSTANT LATERAL IMPULSE WITH VARIABLE THRUST

R. J. HUNG and Y. T. Long

The University of Alabama in Huntsville

Huntsville, Alabama 35899, USA

(NASA-CR-200046) BUBBLE MASS CENTER AND FLUID FEEDBACK FORCE FLUCTUATIONS ACTIVATED BY CONSTANT LATERAL IMPULSE WITH VARIABLE THRUST (Alabama Univ.) 27 p

N96-17859

Unclas

G3/18 0098277

Abstract

Sloshing dynamics within a partially filled rotating dewar of superfluid helium II are investigated in response to constant lateral impulse with variable thrust. The study, including how the rotating bubble of superfluid helium II reacts to the constant impulse with variable time period of thrust action in microgravity, how amplitudes of bubble mass center fluctuates with growth and decay of disturbances, and how fluid feedback forces fluctuates in activating on the rotating dewar through the dynamics of sloshing waves are investigated. The numerical computation of sloshing dynamics is based on the non-inertial frame spacecraft bound coordinate with lateral impulses actuating on the rotating dewar in both inertial and non-inertial frames of thrust. Results of the simulations are illustrated.

I. Introduction

In order to carry out scientific experiments, some experimental spacecraft use cryogenic cooling for observation instrumentation and telescope, superconducting sensors for gyro read-out and maintain very low temperatures near absolute zero for mechanical stability. The approaches to both cooling and control involve the use of helium II. In this study, the response of cryogenic systems to sloshing dynamics actuated by constant impulses with variable thrusts are investigated. Illistrations specific to the Gravity Probe-B (GP-B) spacecraft are presented. The GP-B spacecraft adopts the cooling and boil-off from the cryogenic liquid helium dewar as a cryogen and propellant to maintain the cooling of instruments, attitude control and drag-free operation of the spacecraft. Potential fluid management problems may arise due to asymmetric distribution of liquid helium and vapor or to perturbations in the free surface.

For the case of the GP-B spacecraft, cryogenic liquid helium II, at a temperature of 1.8 K, is used as the propellant. With its superfluid behavior, there is very small temperature gradient in the liquid helium. In the negligibly small temperature gradient along the surface which drive Marangoni convection, the equilibrium shape of the free surface is governed by a balance of capillary, centrifugal and gravitational forces. Determination of liquid-vapor interface profiles based on computational experiments can uncover details of the flow which can not be easily visualized or measured experimentally in a microgravity environment.

The instability of the liquid-vapor interface can be induced by the presence of longitudinal and lateral impulses. Thus, slosh waves are excited, producing high and low frequency oscillations in the liquid propellant. The

sources of the residual accelerations include effects of the Earth's gravity gradient and g-jitter. A recent study[1] suggests that the high frequency accelerations may be unimportant in comparison with the residual motions caused by low frequency accelerations.

The time-dependent behavior of partially-filled rotating fluids in reduced gravity environments was simulated by numerically solving the Navier Stokes equations subject to the initial and boundary conditions[2-6]. At the interface between the liquid and the gaseous fluids, both the kinematic surface boundary condition and the interface stress conditions for components tangential and normal to the interface were applied[2-6]. The initial conditions were adopted from the steady-state formulations developed by Hung et al[7-9]. Some of the steady-state formulations of interface shapes were compared with the available experiments carried out by Leslie[10] in a free-falling aircraft (KC-135). The experiments carried out by Mason et al[11] showed that the classical fluid mechanics theory is applicable to cryogenic liquid helium in large containers.

As the spacecraft moves along its orbit, the fluid is subject to the acceleration that arises from the gravity gradients of the Earth[12-14]. The interaction between the particle mass fluid and the spacecraft due to gravity gradient accelerations[13] are capable of exciting slosh waves which in turn exert forces and moments on the fluid containers and spacecraft. Sources of residual acceleration contributing to g-jitter are also capable of exciting slosh waves on the fluid containers.

The purpose of this paper is to investigate the dynamical behavior of helium II in a rotating cylinder activated by a constant lateral impulse with various thrusts[15-17].

At temperatures close to absolute zero, quantum effects begin to be of

importance in the properties of fluids. At a temperature of 2.17 K, liquid helium has a λ-point (a second-order phase transition); at temperatures below this point, liquid helium (helium II) has a number of remarkable properties, the most important of which is superfluidity. This is the property of being able to flow without viscosity in narrow capillaries or gaps. At temperatures other than zero, helium II behaves as if it were a mixture of two different liquids. One of these is a superfluid and moves with zero viscosity along a solid surface. The other is a normal viscous fluid. The two motions occur without any transfer of momentum from one to another for velocities below a critical velocity[15-17]. For the components of normal and superfluid velocities above a critical velocity, the two fluids are coupled[15-17].

The key parameter of critical velocity to distinguish one-fluid from two-fluid models is a function of fluid temperature and container size. In other words, in considering the dynamical behavior of helium II in a large rotating cylinder, a mixture of the superfluid and the normal fluid without separation of the two fluids is accounted for in the model computation. Density concentration of superfluid is a function of temperature, which is also true for the surface tension and viscous coefficient for helium II[18-20]. In this study, the theory of viscous Newtonian fluids is employed with modification of transport coefficients adjusted by normal and superfluid density concentration which is a function of temperature.

In this paper, the response of superfluid helium II to constant lateral impulse with variable thrust is studied. The effect of the variations of thrust (or the variations the time period of thrust) acting on the dewar with constant lateral impulses in bubble mass center oscillations and the fluid feedback forces due to bubble deformations and oscillations activating on the rotating dewar are

investigated.

II. Non-Inertial Frame Mathematical Formulation of Fundamental Equations

Consider a closed circular dewar partially filled with helium II while the rest of the ullage is filled with helium vapor. The whole fluid system is spinning in the axial direction z of cylindrical coordinates (r, θ, z), with corresponding velocity components (u, v, w). The governing equations for non-inertial frame spacecraft bound coordinates spinning along its z-axis has been given in our recent studies[21-23]. In other words, dynamical forces, such as gravity gradient, g-jitter, and angular accelerations, and centrifugal, Coriolis, surface tension, viscous forces, etc., are given explicitly in the mathematical formulations[21-23]. In the computation of fluid forces, moments, viscous stress and angular momentum acting on the container wall of the spacecraft, one must consider those forces and moments in the inertial frame rather than in the non-inertial frame[21-23].

For the purpose of solving sloshing dynamic problems of liquid propellent systems in orbital spacecraft under a microgravity environment, one must solve the governing equations[21-23] accompanied by a set of initial and boundary conditions. A detailed illustration of these initial and boundary conditions concerning the sloshing dynamics of fluid systems in microgravity was precisely given in Hung and Pan[22,24]. The computational algorithm applicable to cryogenic fluid management under microgravity is also given in Hung et al[25,26]. In this study, in order to show a realistic example, a full scale GP-B spacecraft propellant dewar tank with an outer radius of 78 cm, and an inner radius of 13.8 cm, top and bottom radius of 110 cm and a height of 162 cm has been used in the numerical simulation. The dewar tank is 60% filled with cryogenic liquid helium and the rest of the ullage is filled with helium vapor. The temperature of

cryogenic helium is 1.8 K. In this study the following data were used: liquid helium density = 0.146 g/cm^3, helium vapor density = 0.00147 g/cm^3, fluid pressure = 1.66 x 10^4 dyne/cm^2, surface tension coefficient at the interface between liquid helium and helium vapor = 0.353 dyne/cm, liquid helium viscosity coefficient = 9.61 x 10^{-5} cm^2/s; and contact angle = 0°. The initial profiles of the liquid-vapor interface for the rotating dewar are determined from computations based on algorithms developed for the steady state formulation of microgravity fluid management[2,26,27].

A staggered grid for the velocity components is used in this computer program. MAC (marker-and-cell) method[28] of studying fluid flows along a free surface is adopted. VOF (volume of fluid) method is used to solve finite difference equations numerically. Approximate flow velocity is calculated from the explicit approximation of momentum equations based on the results from the previous time step. Computation of pressure and velocity at the new time step are, thus, obtained from iteratively solving pressure equation through conjugate residual technique[29-32]. Configuration of liquid-vapor interface adjusted by the surface tension effect at the new time step are then finally obtained. The time step during this computation is automatically adjusted through the fulfillment of the stability criteria of computed grid size. Convergence criterion of the iteration of pressure equation is based on the computed velocity at each cell which shall satisfy continuity equation with the errors no more than 10^{-5} of the velocity difference[33]. As for the volume conservation of liquid, a deviation of less than 1 % error of volume is always guaranteed before a move to the next time step. Figs. 1(A), (B), and (C) show initial shape of rotating bubble in three-dimensional profile, the distribution of grid points for the dewar in the radial-axial plane and radial-circumferential plane, respectively, in cylindrical

coordinates.

III. Microgravity Sloshing Dynamics Response to Constant Lateral Impulse with Various Magnitudes of Thrust Acting on Rotating Dewar

By using the mathematical formulations illustrated in the previous sections, one can numerically simulate microgravity sloshing dynamics associated with spinning motion. An example is given to illustrate sloshing dynamics in response to constant lateral impulse with various magnitudes of thrust during the time period of guidance and/or attitude controls. The dewar container of the GP-B is spinning with a rotating rate of 0.1 rpm during its normal operation. In this study, with the following lateral impulses are assumed:

(a) Constant lateral impulse per unit mass is 10^{-4} g_o•s where g_o (-9.81 m/s^2) is the Earth's gravitational acceleration.

(b) Time period of thrust acting on the dewar is Δt.

(c) Forms of lateral impulsive (thrust) accelerations acting on non-inertial frame are

$$\hat{a}=[a_x, a_y, a_z]=[1,0,0]\,a_{gj} \quad \textit{in cartesian coordinate}$$

$$\hat{a}=[a_r, a_\theta, a_z]=[\cos\theta, -\sin\theta, 0]\,a_{gj} \quad \textit{in cylindrical coordinate}$$

both for $0 \le t \le \Delta t$

$$\textit{and } \hat{a}=[0,0,0] \quad \textit{for } t<0 \textit{ and } t>\Delta t$$

Table 1 shows the cases of variable magnitudes of thrust (or variable time periods of thrust) with constant lateral impulses acting on rotating dewar considered in this study. Cases A to F show the thrust with a value of 10^{-5}, 2×10^{-6}, 10^{-6}, 5×10^{-7}, 2.5×10^{-7}, and 2×10^{-7} g_o, respectively, acting on the dewar container.

The time evolution of the bubble (liquid-vapor interface) oscillations in

response to the constant lateral impulses with various magnitudes of thrust are investigated. Figure 2 shows the time sequence evolution of three dimensional rotating bubble oscillations. The figure shows bubble oscillations at times t=0.00 (shown in Figure 1), 209, 409, and 1980s. It shows that a greater bubble deformation is resulted for a greater value of thrust acting on the dewar than that for a smaller value of thrust even though the values of lateral impulses are constant.

Figure 3 shows the time sequence of the bubble oscillation profiles in the vertical r-z plane at θ = 0° and 180° for the similar cases as that shown in Figure 2. It indicates that the horizontal cross-section of the doughnut-shape bubble was pushed to the left (liquid to the right), then to the right (liquid to the left) and vise versa during the course of oscillation in response to the lateral impulses acting on the rotating dewar in positive x-direction.

As indicated earlier, two kinds of lateral impulses, one acting on inertial frame and the other on non-inertial frame (dewar-bound frame), are activated on the rotating dewar. Figures 4 and 5 show the time evolution of growth and decay of the bubble mass center fluctuating amplitudes driven by lateral impulses acting on non-inertial frame and inertial frame, respectively, with rotating dewar. Sub figure (A) and (B) are bubble mass center fluctuations along x- and y-axes, respectively, in dewar-bound coordinates shown in Figures 4 and 5. Comparison of Figures 4 and 5 for bubble mass center fluctuations in response to constant lateral impulses acting on rotating dewar in inertial or non-inertial frames with various magnitudes of thrust are resulted as follows: (a) There is not much difference in terms of the excited wave periods of bubble mass center fluctuations between lateral impulses acting on dewar in inertial and non-inertial frames with various magnitudes of thrust. (b) Wave periods of bubble

mass center fluctuations vary from 280 s for disturbances driven by thrust with 10^{-5} g_o (or time period of thrust with 10 s) and to 500 s for disturbances driven by thrust with 2×10^{-7} g_o (or time period of thrust with 500 s) acting on rotating dewar at the beginning of bubble fluctuations. In other words, longer wave periods of bubble mass center fluctuations are excited for lower thrust (or longer time period of thrust) acting on the dewar than that with shorter wave periods of bubble mass center oscillations are induced for higher thrust (or shorter time period of thrust) activating on the dewar. (c) Wave periods of bubble mass center fluctuations prolong from 480 s for disturbances driven by thrust with 10^{-5} g_o to 680 s for disturbances driven by thrust with 2×10^{-7} g_o acting on the dewar with smaller amplitudes near the end of bubble fluctuations. (d) There are some differences in terms of the excited wave amplitudes of bubble mass center fluctuations between lateral impulses acting on dewar in inertial and non-inertial frames with various magnitudes of thrust. To be specific for the maximum amplitudes of the excited bubble mass center fluctuations, there are (1.8 cm, 0.3 cm) for 500 s time period of thrust, (2.3 cm, 1.2 cm) for 400 s time period of thrust, (3.2 cm, 2.5 cm) for 200 s time period of thrust, and (3.4 cm, 3.0 cm) for 10 s time period of thrust corresponding to amplitudes excited by thrust acting on the rotating dewar in (inertial frame, non-inertial frame). In other words, thrust acting on rotating dewar in inertial frame always excite greater amplitude of bubble mass center fluctuations than that of amplitudes induced by thrust acting on rotating dewar in non-inertial frame. It is also true that a longer time period of thrust acting on the dewar can excite a greater deviation of bubble mass center fluctuations between that associated with inertial and non-inertial frames than that of shorter period of thrust acting on the dewar. This is due to the fact that a longer period of thrust acting on the

dewar in inertial frame is equivalent to the thrust acting on a wider range of fluids in the rotating dewar which induces a disturbance of collective oscillations resulting in a greater maximum amplitude fluctuations. (e) Lateral impulses with a greater thrust acting on the dewar can excite a greater magnitude of bubble mass center fluctuations than that of a smaller thrust acting on the dewar. (f) Constant lateral impulses with various strengths of thrust excite a greater amplitude of bubble mass center fluctuations associated with a higher strength of thrust at the very beginning. The characteristics of this mass center fluctuations with a higher dissipation rate for a greater amplitude mode makes the time period of dissipation with roughly a same value for constant lateral impulses with variable thrusts acting on the dewar in both inertial and non-inertial frames. (g) There are some delay time between time period of thrust acting on the dewar and the time of bubble mass center fluctuations which reach to its peak value. Times at which bubble mass center reach to their peak values are 120, 170, 300, 650, 1020 and 1180 s for time periods of thrust acting on the dewar with 10, 50, 100, 200, 400, and 500 s.

A comparison of Figures 4 and 5 also illustrates some peculier behavior of cryogenic helium fluids with temperature below λ-point (2.17 k) in which helium demonstrates a number of remarkable properties of superfluidity such as extremely low viscous and surface tension coefficients in response to constant lateral impulses with various thrust in a microgravity environment. It can be concluded as follows: (a) There is a great time delay between the ending time of impulse acting on the dewar and time of bubble mass center fluctuations reaching their peak values. (b) Proportionality of time delay to time period of thrust acting on the dewar is greater for a greater thrust acting on the dewar while the value of time delay between the time reaching their peak values of mass center

fluctuations and the ending time of impulse acting on the dewar is greater for longer time period of thrust acting on the dewar. (c) The displacement of bubble mass center was sinusoidally shifting continuously even long after the ending of the impulse. Because of extremely low surface tension and viscosity for helium II fluids, the oscillations of the bubble mass center fluctuations continued for a long period of time and exponentially decaying out finally.

Figures 6 and 7 show the time evolution of the growth and decay of interactive fluid feedback forces due to bubble deformations and oscillations activating on the rotating dewar in response to lateral impulses acting on the dewar in non-inertial and inertial frames, respectively. Subfigures (A) and (B) are fluid feedback force fluctuations along x- and y-axes, respectively, in dewar-bound coordinates shown in Figures 6 and 7. Comparison of Figures 6 and 7 for fluid feedback forces fluctuations due to bubble deformations and oscillations in response to constant lateral impulses acting on the rotating dewar in inertial or non-inertial frames with various magnitudes of thrust are resulted as follows: (a) In contrast to bubble mass center fluctuations with delay time, an immediate reaction is observed for fluid feedback force activating on the dewar due to bubble deformations in response to the lateral impulses. (b) Wave periods of fluid feedback force fluctuations are very much similar to that of the wave periods of bubble mass center fluctuations in response to the lateral impulses. (c) Similar to bubble mass center fluctuations, longer wave periods of fluid feedback force fluctuations are excited for lower thrust acting on the dewar than that with shorter wave periods of fluid feedback force fluctuations are induced for higher thrust activating on the dewar. (d) It is also true that wave periods of fluid feedback force fluctuations became longer at the end of oscillations than that were excited right at the beginning of lateral impulses

acting on the dewar. (e) There are some differences in terms of the excited wave amplitudes of fluid feedback force fluctuations acting on the dewar in inertial and non-inertial frames with variable thrusts. To be specific for the maximum amplitudes of the fluid feedback force fluctuations, there are (90, 20) dynes for 500 s time period of thrust, (115, 60) dynes for 400 s time period of thrust, (205, 160) dynes for 200 s time period of thrust, (260, 220) dynes for 100 s time period of thrust, (340, 315) dynes for 50 s time period of thrust, (402, 395) dynes for 10 s time period of thrust corresponding to amplitudes excited by thrust acting on the dewar in (inertial frame, non-inertial frame). In other words, thrust acting on rotating dewar in inertial frame always excite greater amplitude fluid feedback force fluctuations than that of amplitudes induced by thrust acting on rotating dewar in non-inertial frame. It is also true that a longer time period of thrust acting on the dewar can excite a greater deviation of fluid feedback force fluctuations between that associated with inertial and non-inertial frames than that of shorter time period of thrust acting on the dewar.

IV. Discussion and Conclusion

Sloshing dynamics of spacecraft disturbances in response to constant lateral impulse with variable thrust due to the activation of guidance and/or attitude controls of spacecraft operation[3] in microgravity have been investigated. In this study, the effect of surface tension on partially-filled rotating dewar (liquid helium and helium vapor) activated by the time-dependent constant lateral impulse with variable thrust in inertial and non-inertial frames of rotating dewar have been carried out. Study is based on the computation of three-dimensional non-inertial frame Navier-Stokes equations subject to the initial and boundary conditions[21,22]. The initial condition for the liquid-vapor

interface profiles were adopted from the steady-state formulation of rotating dewar developed by Hung and Leslie[27] and by Hung et al[8].

In this study, the time evolution of the sloshing dynamics governed liquid-vapor interface bubble oscillations in response to constant lateral impulse with variable thrusts have been investigated. The simulation of both bubble mass center and fluid feedback force fluctuations due to the bubble deformations show that the greater the thrust, the greater the amplitudes of fluctuations are resulted. There is some delay time between the ending of thrust acting on the dewar and the time of bubble mass center fluctuations reaching their peak values. On the contrary to delay time for bubble mass center fluctuations, there is an immediate reaction resulted for fluid feedback force acting on the dewar in response to the lateral impulse. Comparison for both the amplitudes of bubble mass center and fluid feedback force fluctuations due to bubble deformations for variable thrusts in inertial and non-inertial frames acting on the dewar show that the amplitudes of the fluctuations driven by thrust acting on the dewar in inertial frame are always greater than that driven by thrust acting on the dewar in non-inertial frame.

Because of the peculiar physical properties of cryogenic liquid helium[15-20], extremely low values of surface tension and viscosity coefficient of the materials make oscillations of bubble and sloshing dynamics modulated fluctuating fluid feedback forces actuated on the container in response to the lateral impulsive acceleration continue for a long period of time and gradually decay exponentially. In this research, it has demonstrated how the amplitude of cryogenic helium sloshing dynamics disturbances grow and decay in response to the lateral impulsive acceleration in microgravity. A full understanding of the time history of growth and decay of disturbances is important for the design of

guidance and attitude controls of spacecraft utilizing cryogenic liquid systems[3,15-20,34].

Acknowledgement

The authors appreciate the support received from the National Aeronautics and Space Administration through the NASA Grant NAG8-938 and NASA contract NAS8-39609/Delivery Order No. 103. They would like to express their gratitude to Richard A. Potter of NASA/Marshall Space Flight Center for the stimulating discussions during the course for the present study.

References

1. Kamotani, Y.; Prasad, A.; Oastrach, S.: Thermal Convection in an Enclosure Due to Vibrations Aboard a Spacecraft, AIAA Journal,19 (1981) 511-516.
2. Hung, R.J.; Shyu, K.L.: Liquid Hydrogen Suction Dip and Slosh Wave Excitation During Draining Under Normal and Reduced Gravity Environment, Transactions of the Japan Society for Aeronautical and Space Sciences,36 (1994) 217-233.
3. Hung, R.J.; Lee, C.C.; Leslie, F.W.: Spacecraft Dynamical Distribution of Fluid Stresses Activated by Gravity Jitters Induced Slosh Waves, Journal of Guidance, Control and Dynamics,15 (1992) 817-824.
4. Hung, R.J.; Lee, C.C.; Leslie, F.W.: Similarity Rules in Gravity Jitter-Related Spacecraft Liquid Propellant Slosh Wave Excitation, Journal of Fluids and Structures,6 (1992) 493-522.
5. Hung, R.J.; Long, Y.T.; Pan, H.L.: Sloshing Dynamics Induced Angular Momentum Fluctuations Driven by Jitter Accelerations Associated with Slew Motion in Microgravity, Transactions of the Japan Society for Aeronautical and Space Sciences,37 (1994) 217-233.
6. Hung, R.J.; Lee, C.C.: Effect of Baffles on Imbalance Bubble Configurations Due to Sloshing Dynamics Driven by Gravity Gradient Acceleration in Microgravity, Canadian Aeronautics and Space Journal,40 (1994) 185-202.
7. Hung, R.J.; Lee, C.C.; Leslie, F.W.: Dynamic Characteristics of the Partially Filled Rotating Dewar of Gravity Probe-B Spacecraft, Acta Astronautica,32 (1994) 199-209.
8. Hung, R.J.; Tsao, Y.D.; Hong, B.B.; Leslie, F.W.: Bubble Behavior in a Slowly Rotating Helium Dewar in Gravity Probe-B Spacecraft Experiments, Journal of Spacecraft and Rockets,26 (1989) 167-172.
9. Hung, R.J.; Tsao, Y.D.; Hong, B.B.; Leslie, F.W.: Dynamical Behavior of

Surface Tension on Rotating Fluids in Low and Microgravity Environments, International Journal for Microgravity Research,11 (1989) 81-95.

10. Leslie, F.W.: Measurements of Rotating Bubble Shapes in a Low Gravity Environment, Journal of Fluid Mechanics,161 (1985) 269-279.
11. Mason, P.; Collins, D.; Petrac, D.; Yang, L.; Edeskuty, F.; Schuch, A.; Williamson, K.: The Behavior of Superfluid Helium in Zero Gravity, Proc. 7th International Cryogenic Engineering Conferences, Surrey, England, Science and Technology Press, 1978.
12. Avuduyevsky, V.S.: (editor), Scientific Foundations of Space Manufactoring, MIR, Moscow, USSR, 1984.
13. Forward, R.L.: Flattening Space-Time Near the Earth, Physical Review,Series(A),26 (1982) 735-744.
14. Misner, C.W.; Thorne, K.S.; Wheeler, J.A.: Gravitation, W.H. Freeman Co., San Francisco, CA, 1973.
15. Van Sciver, S.W.: Helium Cryogenics, Plenium Press, New York, 1986.
16. Donnelly, R.J.: Quantized Vertices in Helium II, Cambridge University Press, Cambridge, 1991.
17. Hung, R.J.; Pan, H.L.; and Long, Y.T.: Peculiar Behavior of Helium II Disturbances Due to Sloshing Dynamics Driven by Jitter Accelerations Associated with Slew Motion in Microgravity, Cryogenics,34 (1994) 641-648.
18. Wilks, H.: The Properties of Liquid and Solid Helium, Clarendon Press, Oxford, 1967.
19. Hoare, F.E.; Jackson, L.C.; Kurt, N.: Experimental Cryogenics: Liquid Helium II , Butterworths, London, 1961.
20. Donnelly, R.J.: Superfluid Turbulence, Scientific American, November (1988) 100-108.

21. Hung, R.J.; Pan, H.L.: Differences in Gravity Gradient and Gravity Jitter Excited Slosh Waves in Microgravity, Transactions of the Japan Society for Aeronautical and Space Sciences,36 (1993) 153-169.

22. Hung, R.J.; Pan, H.L.; Leslie, F.W.: Gravity Gradient or Gravity Jitter Induced Viscous Stress and Moment Fluctuations in Microgravity, Fluid Dynamics Research,14 (1994) 29-51.

23. Hung, R.J.; Pan, H.L.; Leslie, F.W.: Fluid System Angular Momentum and Moment Fluctuations Driven by Gravity Gradient or Gravity Jitter in Microgravity, Z. Fluwiss. Weltraumforsch.,18 (1994) 195-202.

24. Hung, R.J.; Pan, H.L.: Asymmetric Slosh Wave Excitation in Liquid-Vapor Interface Under Microgravity, Acta Mechanica Sinica,9 (1993) 298-311.

25. Hung, R.J.; Lee, C.C.; and Leslie, F.W.: Effect of Baffle on the Spacecraft Fluid Propellant Viscous Stress and Moment Fluctuations, Transactions of the Japan Society for Aeronautical and Space Sciences,35 (1993) 187-207.

26. Hung, R.J.; Lee, C.C.; Leslie, F.W.: Effect of the Baffle on the Asymmetric Gravity-Jitter Excited Slosh Waves and Spacecraft Moment and Angular Momentum Fluctuations, Journal of Aerospace Engineering (United Kingdom),207 (1993) 105-120.

27. Hung, R.J.; Leslie F.W.: Bubble Shapes in a Liquid-Filled Rotating Container Low Gravity, Journal of Spacecraft and Rockets,25 (1988) 70-74.

28. Harlow, F.H.; Welch, F.E.: Numerical Calculation of Time-Dependent Viscous Incompressible Flow of Fluid with Free Surface, Physics of Fluids,8 (1965) 2182-2189.

29. Hirt, C.W.; Nichols, B.D.: Volume of Fluid (VOF) Method for the Dynamics of Free Boundaries, Journal of Computational Physics,39 (1981) 201-225.

30. Salvadori, M.G.; Baron, M.L.: Numerical Methods in Engineering, Prentice-

Hall, Inc., Englewood Cliffs, NJ, 1961.

31. Hageman, L.A.; Young, D.M.: Applied Iterative Methods, Academic Press, New York, 1981.

32. Young, D.: Iterative Methods for Solving Partial Difference Equations of Elliptical Type, Transactions of American Mathematical Society, 76 (1954) 92-111.

33. Patanker, S.V.: Numerical Heat Transfer and Fluid Flow, Hemisphere-McGraw-Hill, New York, NY, 1980.

34. Hung, R.J.; Pan, H.L.: Fluid Force Activated Spacecraft Dynamics Driven by Gravity Gradient and Jitter Accelerations, Journal of Guidance, Control, and Dynamics, 17 (1994) in press.

Table 1 Constant Lateral Impulses with Variable Magnitudes of Thrust Acting on the Rotating Dewar

Case	Thrust (g_0)	Time Period of Thrust Acting on Dewar (s)	Impulse ($g_0 \cdot s$)
A	10^{-5}	10	10^{-4}
B	$2X10^{-6}$	50	10^{-4}
C	10^{-6}	100	10^{-4}
D	$5X10^{-7}$	200	10^{-4}
E	$2.5X10^{-7}$	400	10^{-4}
F	$2X10^{-7}$	500	10^{-4}

Figure Captions

Figure 1 (A) Initial shape of rotating bubble in three-dimensional configuration, (B) distribution of grid points in the radial-axial plane, and (C) in the radial-circumferential plane.

Figure 2 Time sequence evolution of three-dimensional bubble oscillations for rotating dewar in response to constant lateral impulse with variable thrusts in cases (A) to (F).

Figure 3 Time sequence evolution of bubble oscillations for rotating dewar in r-z plane at $\theta = 0°$ and 180°, in response to constant lateral impulse with variable thrusts in cases (A) to (F).

Figure 4 Time sequence evolution of bubble mass center fluctuations in response to constant lateral impulse with variable thrust acting on non-inertial frame. (A) Bubble mass center fluctuations in x-coordinate, and (B) Bubble mass center fluctuations in y-coordinate.

Figure 5 Time sequence evolution of bubble mass center fluctuations in response to constant lateral impulse with variable thrusts acting on inertial frame (A) Bubble mass center fluctuations in x-coordinate and (B) Bubble mass center Fluctuations in y-coordinate.

Figure 6 Time sequence fluid feedback forces fluctuations exerted on the dewar in response to constant lateral impulses with variable thrusts acting on non-inertial frame. (A) Fluid feedback force fluctuations along x-direction, and (B) Fluid feedback force fluctuations along y-direction.

Figure 7 Time sequence fluid feedback force fluctuations exerted on the dewar in response to constant lateral impulses with variable thrusts acting on inertial frame. (A) Fluid feedback force fluctuations along x-direction, and (B) Fluid feedback force fluctuations along y-direction.

(A)

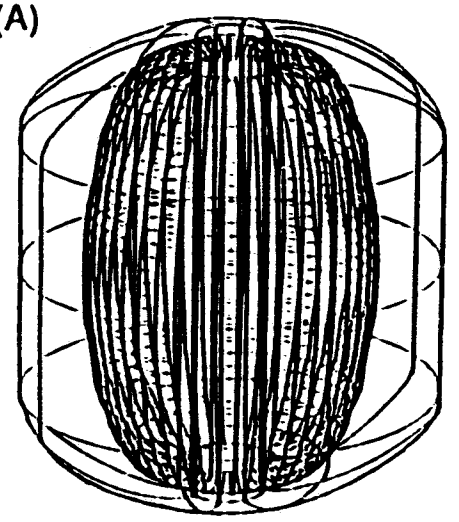

(A) Initial Shape of Rotating Bubble in Three Dimensional Profile

(B) Grid Points in Radial-Axial Direction

(C) Grid Points in Radial-Circumferetial Direction

(B)

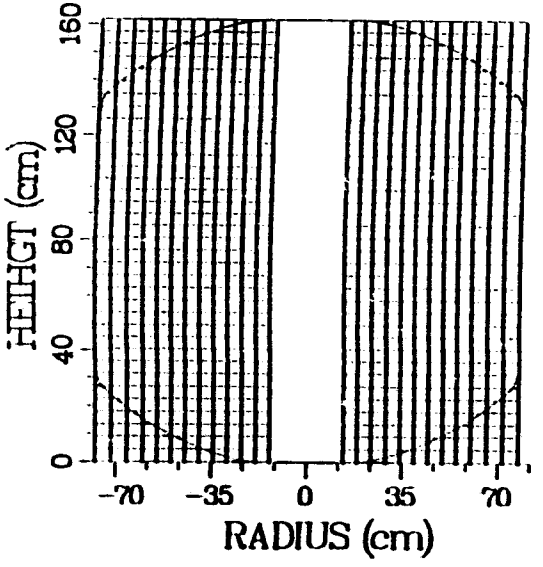

(C)

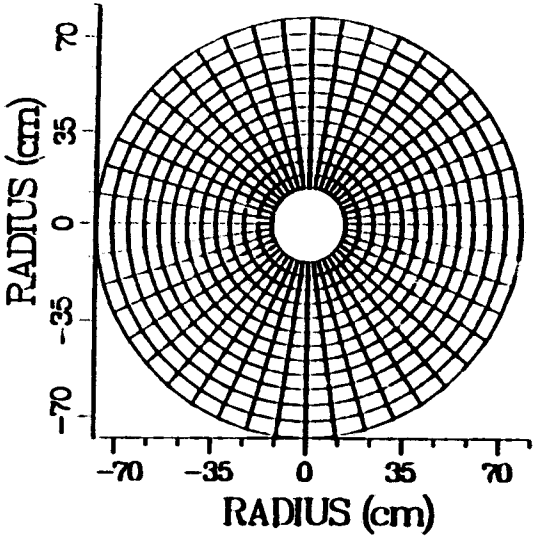

Fig. 1

THREE DIMENSIONAL LIQUID - VAPOR INTERFACE OSCILLATIONS

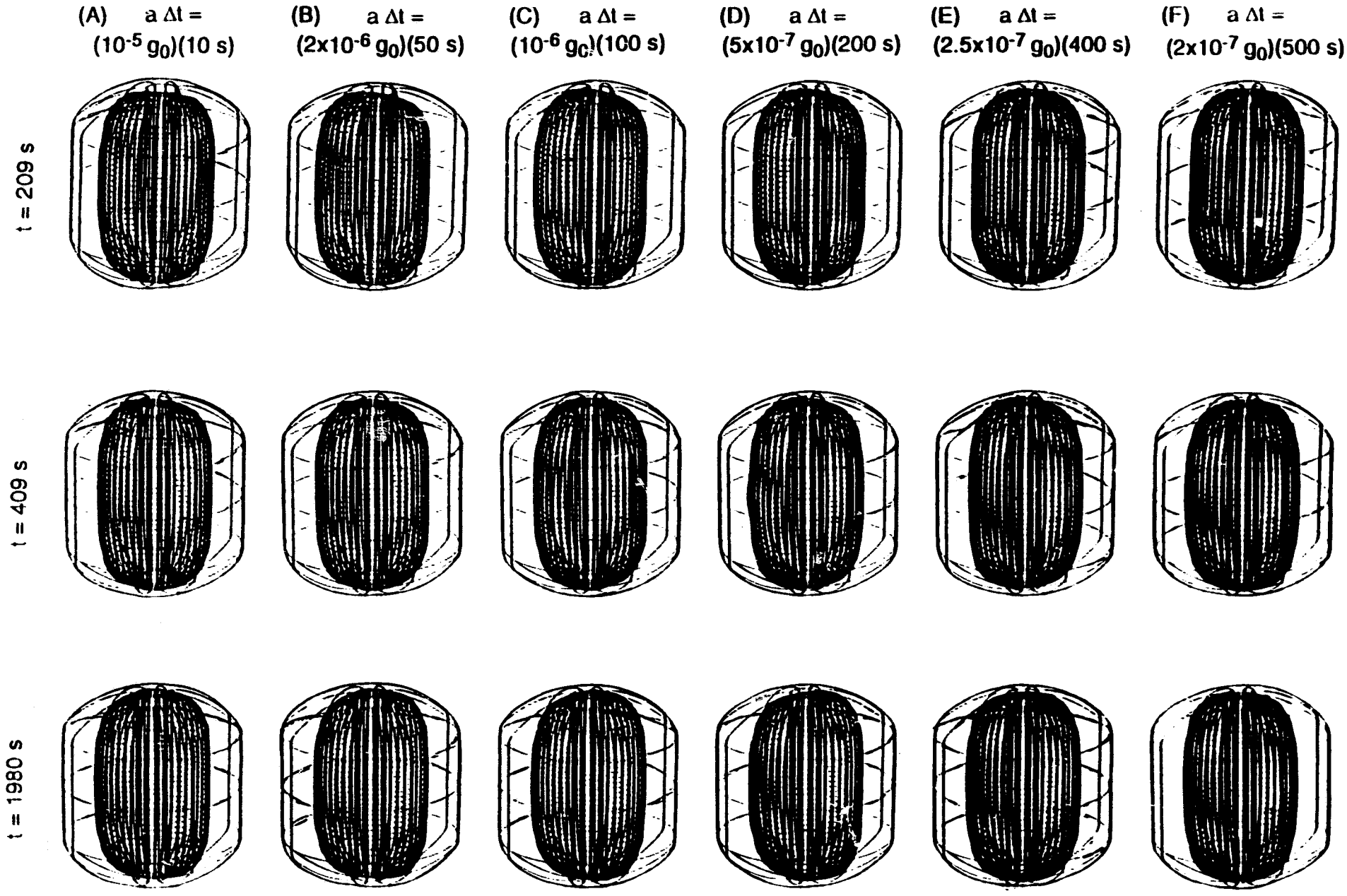

Fig. 2

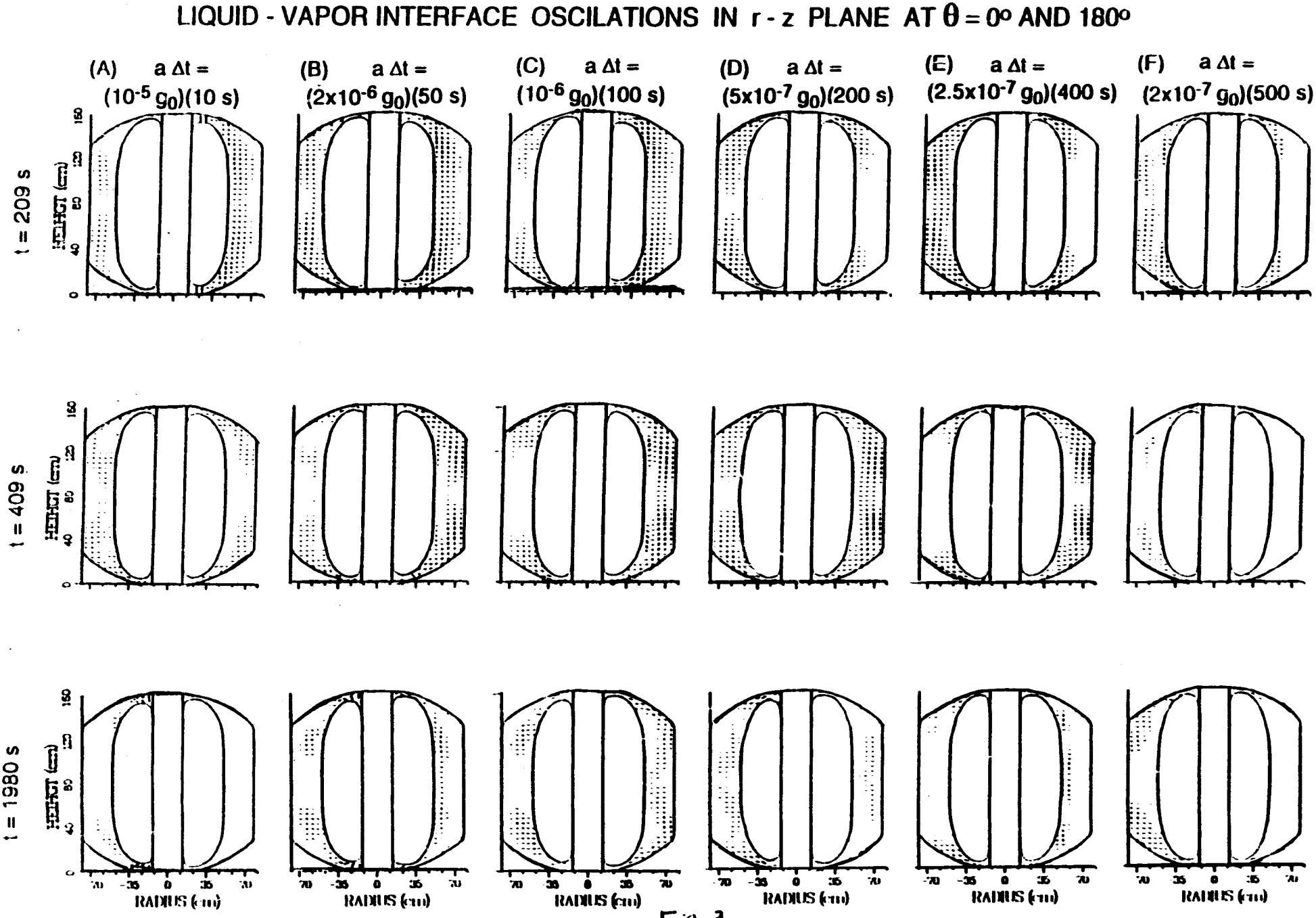
LIQUID - VAPOR INTERFACE OSCILATIONS IN r - z PLANE AT θ = 0° AND 180°
(A) a Δt = (10⁻⁵ g₀)(10 s)
(B) a Δt = (2x10⁻⁶ g₀)(50 s)
(C) a Δt = (10⁻⁶ g₀)(100 s)
(D) a Δt = (5x10⁻⁷ g₀)(200 s)
(E) a Δt = (2.5x10⁻⁷ g₀)(400 s)
(F) a Δt = (2x10⁻⁷ g₀)(500 s)
t = 209 s
t = 409 s
t = 1980 s
HEIGHT (cm)
RADIUS (cm)

Fig. 3

Lateral Impulses Acting on Dewar-Bound Coordinates

(A) X-Direction Bubble Mass Center Fluctuations With Various Time Impulse

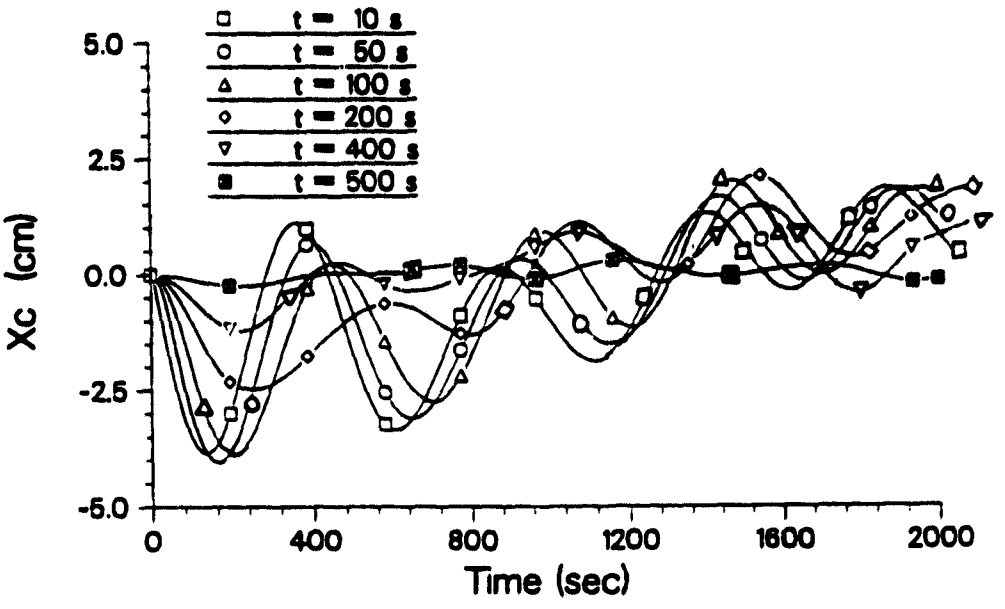

(B) Y-Direction Bubble Mass Center Fluctuations With Various Time Impulse

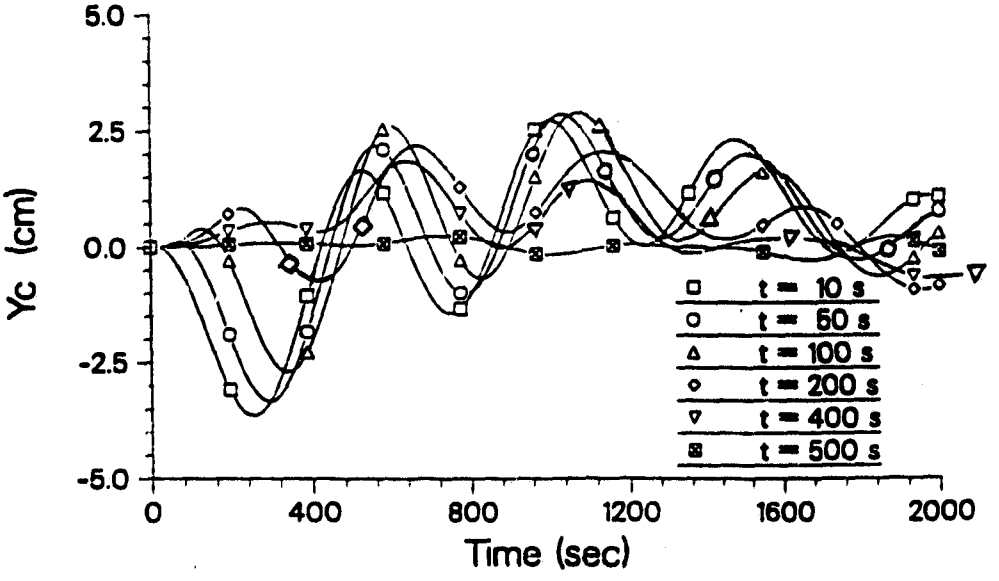

Fig 4

Lateral Impulses Acting on Inertial Coordinates

(A) X-Direction Bubble Mass Center Fluctuations With Various Time Impulse

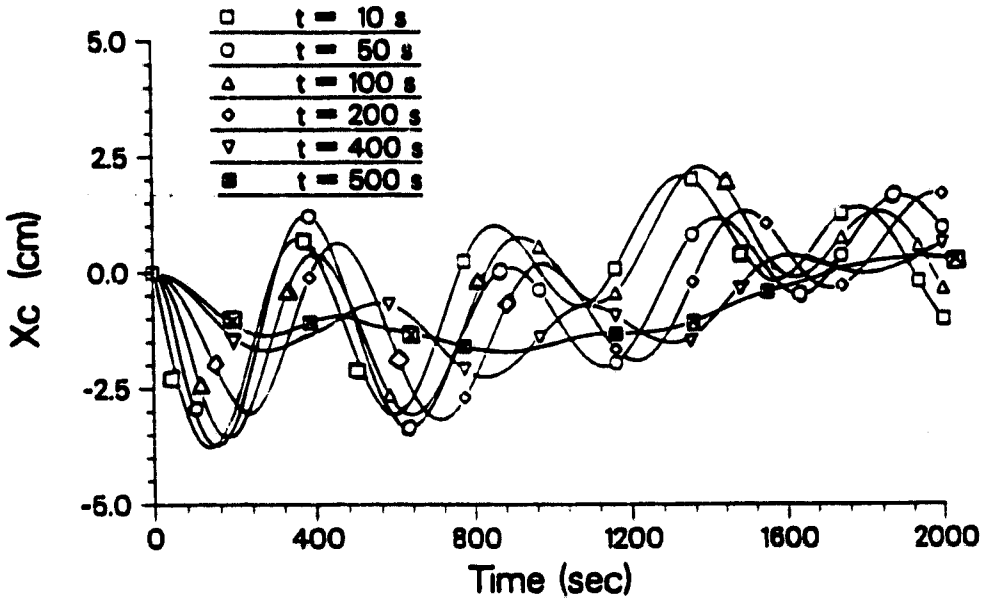

(B) Y-Direction Bubble Mass Center Fluctuations With Various Time Impulse

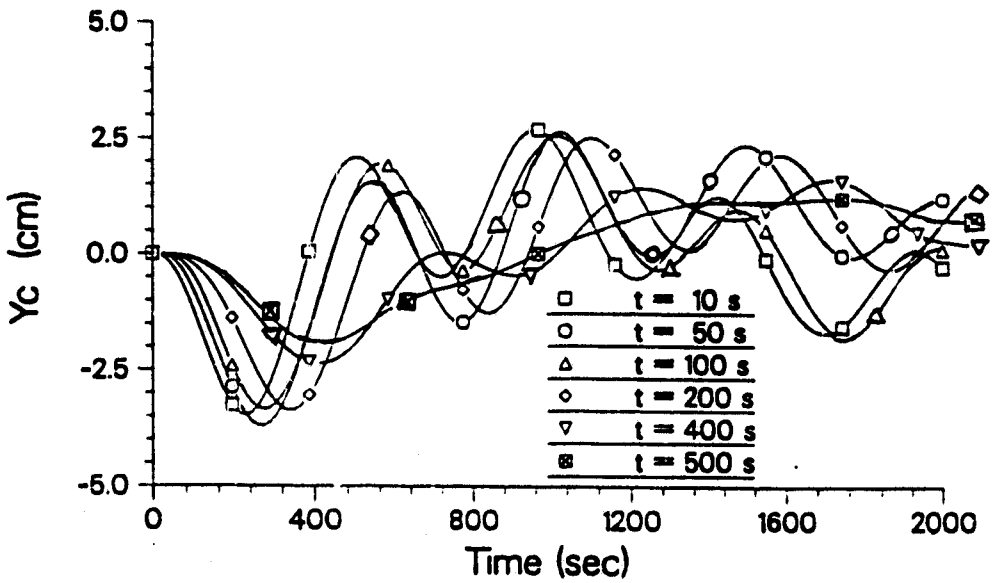

Fig 5

Lateral Impulses Acting on Dewar-Bound Coordinates

(A) X-Direction Fluid Feedback Forces Exerted on The Rotating Dewar

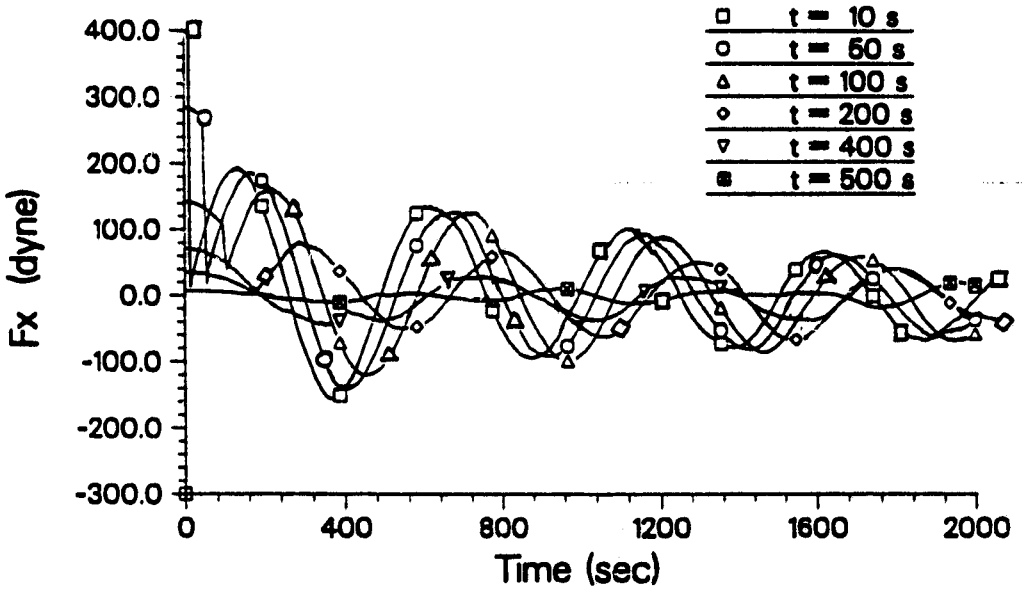

(B) Y-Direction Fluid Feedback Forces Exerted on The Rotating Dewar

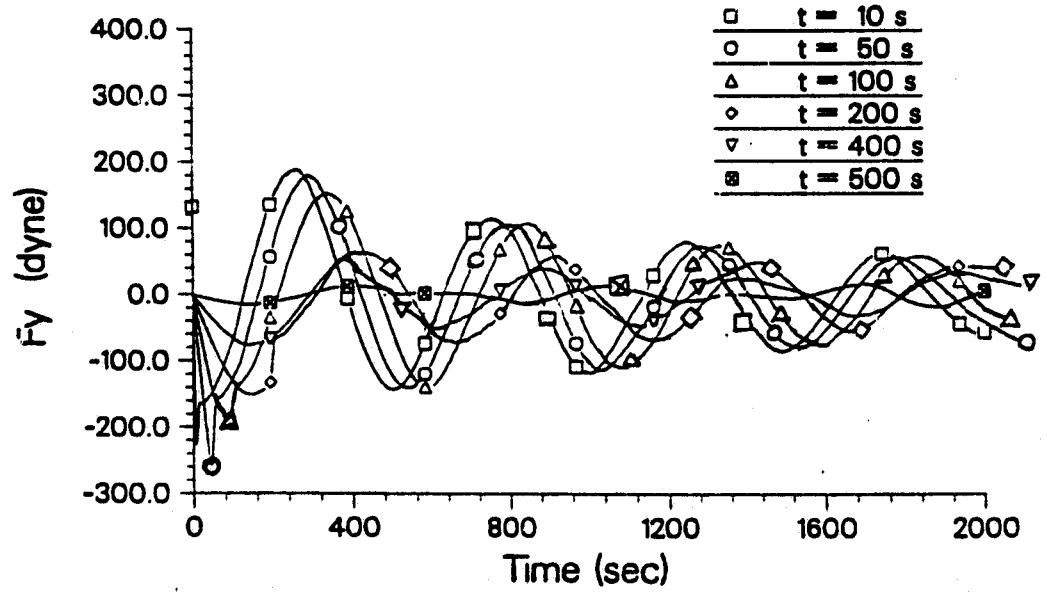

Fig. 6

Lateral Impulses Acting on Inertial Coordinates

(A) X-Direction Fluid Feedback Forces Exerted on The Rotating Dewar

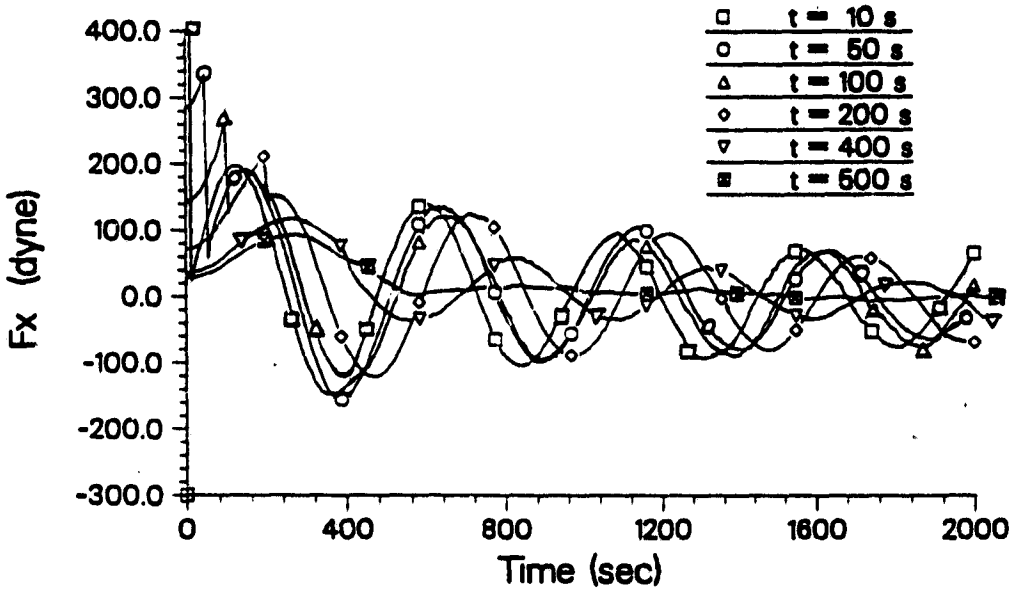

(B) Y-Direction Fluid Feedback Forces Exerted on The Rotating Dewar

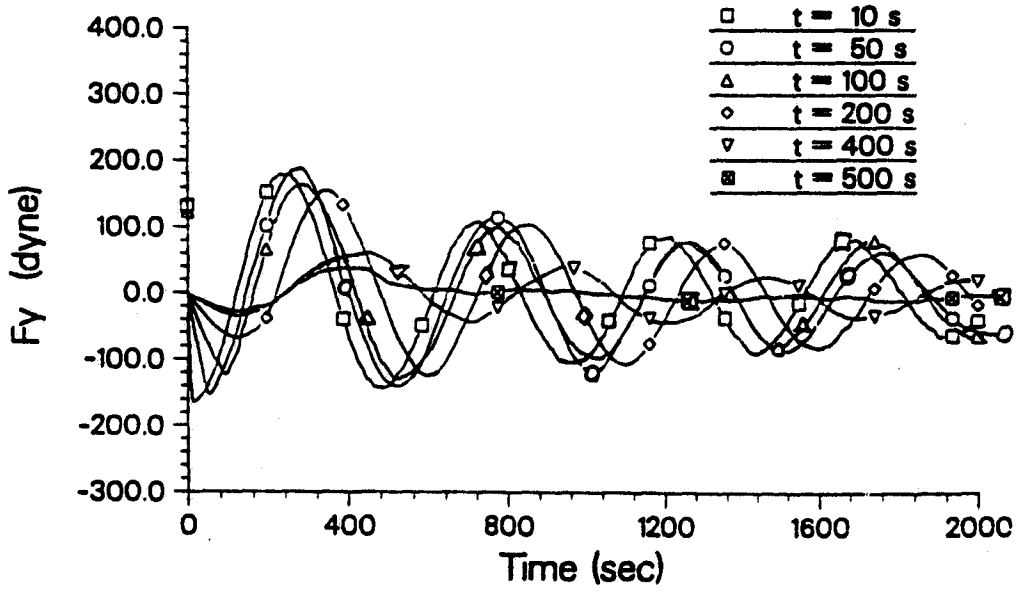

Fig. 7